JOURNAL OF GEOPHYSICAL RESEARCH, VOL. 112, E09005, doi:10.1029/2006JE002873, 2007

Trends in effusive style at the Tharsis Montes, Mars, and implications for the development of the Tharsis province

Jacob E. Bleacher,[1,2] Ronald Greeley,[1] David A. Williams,[1] Shelby R. Cave,[1] and Gerhard Neukum[3]

Received 29 November 2006; revised 24 April 2007; accepted 23 May 2007; published 19 September 2007.

[1] We mapped lava flows on the Tharsis Montes (Arsia Mons, Pavonis Mons, and Ascraeus Mons) using High Resolution Stereo Camera images that centrally transect each shield from north to south, covering ~20% of each shield's surface. These data were co-registered to Mars Orbiter Laser Altimeter, Thermal Emission Imaging System, and Mars Orbiter Camera data, enabling lava flow structures and vents to be consistently differentiated across each volcano. Lava flow and vent abundances and relationships are used to provide new insight into the late Amazonian eruptive history of the Tharsis Montes. The volcanoes are divided into their main flanks, rift aprons, and small-vent fields. Where present on the main flanks, channel-fed flows always embay tube-fed flows, indicating a change from long-lived, stable tube-forming eruption conditions to shorter-lived, less stable channel-forming eruption conditions. Superposition relationships suggest that main flank and rift apron development were likely separated by an eruptive hiatus. The rift aprons, as compared to the main flanks, show higher abundances of tube- and channel-fed flows, and embayment of tube-fed flows by channel-fed flows is less consistent. Several trends from the Arsia Mons, to Ascraeus Mons, southwest rift aprons and small-vent fields were identified, including increased tube abundance, median slope, and number of satellitic eruptive vents and a decrease in channel- to tube-fed flow ratios, apron volumes, and maximum apron elevations. These trends suggest that the most recent volcanic activity at the Tharsis Montes might have originated from a single, shared magma source, possibly marking a change in magma production style from main flank construction.

Citation: Bleacher, J. E., R. Greeley, D. A. Williams, S. R. Cave, and G. Neukum (2007), Trends in effusive style at the Tharsis Montes, Mars, and implications for the development of the Tharsis province, *J. Geophys. Res.*, *112*, E09005, doi:10.1029/2006JE002873.

1. Introduction

[2] The Tharsis Montes, Arsia Mons, Pavonis Mons, and Ascraeus Mons (hereafter referred to as Arsia, Pavonis and Ascraeus), are three large shield volcanoes that form a northeast-trending chain across the Tharsis rise on Mars [*Carr et al.*, 1977; *Crumpler and Aubele*, 1978] between −20° to 20°N, and 230° to 260°E. *Viking Orbiter* images were used to produce regional geologic maps covering the shields and their surroundings [*Scott and Carr*, 1978; *Scott and Tanaka*, 1981a; *Scott et al.*, 1981a, 1981b, 1981c, 1998; *Scott and Tanaka*, 1986; *Scott and Zimbelman*, 1995] at scales of 1:15M, 1:2M, and 1:1M. Although different styles of lava flow emplacement have long been recognized on Tharsis province volcanoes (e.g., channel-fed versus tube-fed) [*Carr*, 1973; *Greeley*, 1973; *Carr et al.*, 1977; *Greeley and Spudis*, 1981; *Cattermole*, 1987, 1990; *Schneeberger and Pieri*, 1991; *Sakimoto et al.*, 1997] limitations in data resolution have hindered consistent differentiation of the resultant lava flow structures in previous mapping campaigns. This distinction is important because different structures form as a result of different eruptive conditions, lava properties, and ambient variables [*Greeley*, 1977a; *Head et al.*, 1981; *Whitford-Stark*, 1982]. Thus an understanding of the abundance and distribution of different lava flow types should serve as a geologic framework for understanding basaltic volcanic systems [*Head et al.*, 1981]. Because this framework has yet to be established for Mars, the evolution of the Tharsis Montes and their relationship to the development of the Tharsis province are not clearly understood.

[3] Spacecraft are currently acquiring high-resolution images that now enable new insights into the geological evolution of the Tharsis Montes through mapping of lava flows. A rigorous characterization of eruptive vents and lava flows, and their distribution in time and space is essential for characterizing the volcanic evolution of these shields.

[1]School of Earth and Space Exploration, Arizona State University, Tempe, Arizona, USA.
[2]Now at Planetary and Geodynamics Laboratory, NASA Goddard Space Flight Center, Greenbelt, Maryland, USA.
[3]Institute of Geological Sciences, Freie Universitaet, Berlin, Germany.

0148-0227/07/2006JE002873$09.00

Thus the objective of this work was to investigate the most recent effusive activity at Arsia, Pavonis, and Ascraeus by mapping different eruptive vents and flow structures, and characterizing their stratigraphic relationships and abundances using *Mars Express* (MEX) High Resolution Stereo Camera (HRSC) [*Neukum et al.*, 2004a] data that are geometrically rectified to the *Mars Global Surveyor* (MGS) Mars Orbiter Laser Altimeter (MOLA) 128 pixel/degree gridded data record [*Smith et al.*, 1999, 2001, 2003] as our map base. These data are supplemented with MGS Mars Orbiter Camera (MOC) [*Malin et al.*, 1992; *Malin and Edgett*, 2001] and *Mars Odyssey* (MO) Thermal Emission Imaging System (THEMIS) [*Christensen et al.*, 2004] data, which together provide unprecedented regional coverage at high resolution across portions of each of the Tharsis Montes, enabling preliminary interpretations of each volcano's recent eruptive history.

2. Background

[4] The Tharsis Montes are spaced ~700 km apart along a northeast-trending lineament within the Tharsis province [*Carr et al.*, 1977; *Crumpler and Aubele*, 1978]. They were identified as shield volcanoes from analysis of Mariner 9 images [*Masursky et al.*, 1972; *McCauley et al.*, 1972; *Carr*, 1973]. Each shield volcano is ~350–500 km in diameter with a summit caldera complex rising between 8 and 15 km above the surrounding plains, on the basis of MOLA data analysis [*Plescia*, 2004]. A developmental sequence for each volcano was established after analysis of *Viking Orbiter* images (~30–269 m/pixel) including (1) construction of the main shield, (2) outbreak of eruption centers on the northeast and southwest flanks, (3) subsidence of the summit due to evacuation of a magma chamber, and (4) continued eruption along the northeast and southwest rift zones [*Crumpler and Aubele*, 1978]. It was suggested that Arsia was the most, and Ascraeus the least, advanced within the sequence, implying that Arsia is the oldest [*Crumpler and Aubele*, 1978; *Plescia and Saunders*, 1979; *Neukum and Hiller*, 1981; *Hodges and Moore*, 1994].

[5] Both *Mariner 9* [*Carr*, 1975; *Masursky et al.*, 1978] and Viking-based geologic mapping [*Scott and Tanaka*, 1981a, 1981b; *Scott et al.*, 1981a, 1981b, 1981c, 1998; *Scott and Tanaka*, 1986; *Scott and Zimbelman*, 1995] grouped multiple lava flow types on the basis of regional morphological characteristics such as albedo, surface roughness, and clarity of flow margins. The surfaces of these shields are associated with an age of late Amazonian on the basis of crater size-frequency distributions [*Plescia and Saunders*, 1979; *Neukum and Hiller*, 1981; *Neukum et al.*, 2004b; *Werner*, 2005]. Although crater abundances suggest that these surfaces are relatively young, the time period required to build the shields has remained a topic of debate (ranging from billions to potentially as short as millions of years), because of uncertainties about Martian magma production rates [*Wilson et al.*, 2001; *Plescia*, 2004]. As a result, the time period during which shield building eruptions initiated for each volcano is not well constrained.

[6] Basaltic eruptions typically produce channels or tubes that deliver lava to the flow fronts [*Wentworth and Macdonald*, 1953; *Macdonald*, 1956]. Observations of active basaltic flows show that lava tubes tend to form during long-lived, stable eruptions of low-viscosity lavas at low to moderate effusion rates, whereas channels tend to develop during shorter-lived, unstable eruptions of higher viscosity lavas at moderate to high effusion rates [*Greeley*, 1973, 1987; *Holcomb*, 1987; *Rowland and Walker*, 1990; *Peterson et al.*, 1994; *Sakimoto et al.*, 1997; *Kauahikaua et al.*, 1998, 2003; *Heliker et al.*, 1998; *Calvari and Pinkerton*, 1998, 1999; *Calvari et al.*, 2003; *Bailey et al.*, 2006]. The formation of lava tubes increases the potential length of a flow because tube-forming eruptions are typically longer-lived, and tubes insulate the lava [*Swanson*, 1973; *Malin*, 1980; *Keszthelyi*, 1995; *Sakimoto and Zuber*, 1998].

[7] The relationship between eruptive conditions and lava flow morphology enabled a determination that Kilauea Volcano, Hawaii, experienced longer-lived, stable eruptions in the Holocene compared to Mauna Loa, which displays fewer tube-fed flows on its current surface [*Greeley*, 1987; *Holcomb*, 1987; *Lockwood and Lipman*, 1987]. Although mapping of lava flows proved useful for understanding other shield volcanoes [*Rowland*, 1996], a similar approach has not been systematically applied to the Tharsis Montes because previous data lack a combination of sufficient spatial resolution to resolve different lava flow structures over large areas for regional mapping. However, the recent acquisition of new image data (HRSC, THEMIS, MOC) enable a characterization of the latest effusive activity through lava flow mapping.

3. Methods

[8] Mapping was conducted along transects through the Tharsis Montes (Figure 1) corresponding to HRSC images H1904 (Arsia), H0891 and H0902 (Pavonis), and H0068 (Ascraeus) [*Neukum et al.*, 2004a]. Each image has a width of 60 to 120 km at a resolution between 13 and 25 m/pixel in the nadir filter, and together cover ~20% of each shield. Several images include two stereo filters (at half the nadir resolution), and four color filters (at 1/4 nadir resolution), all of which collected data simultaneously, providing an unprecedented combination of high resolution with regional coverage [*Neukum et al.*, 2004a]. Using the Video Image Communication And Retrieval (VICAR) software package (http://www-mipl.jpl.nasa.gov/external/vicar.html) (modified by the German Aerospace Center (DLR)), we projected each image into a sinusoidal, orthographic projection with central meridians of 239.5° (Arsia), 247.7° (Pavonis), and 255.5° (Ascraeus). We projected THEMIS and MOC images with the Integrated Software for Imagers and Spectrometers (ISIS) software (http://isis.astrogeology.usgs.gov/index.html) into the same projection. We used ArcGIS 9.1 by ESRI (Environmental Systems Research Institute, Inc.) to place the MOLA grid in a corresponding projection. Well established criteria for mapping lava flow types on Mars and Earth [*Carr*, 1973; *Greeley*, 1973, 1987; *Carr et al.*, 1977; *Carr and Greeley*, 1980; *Greeley and Spudis*, 1981; *Holcomb*, 1987; *Mouginis-Mark et al.*, 1992; *Morris and Tanaka*, 1994; *Rowland*, 1996] served as our basis to map lava tubes, leveed channels, and eruptive vents (Figure 2).

[9] We used the GIS software to derive volcano volume and slope [*Burrough and McDonell*, 1998; *Longley et al.*, 2001] from the MOLA topography data. This enables an

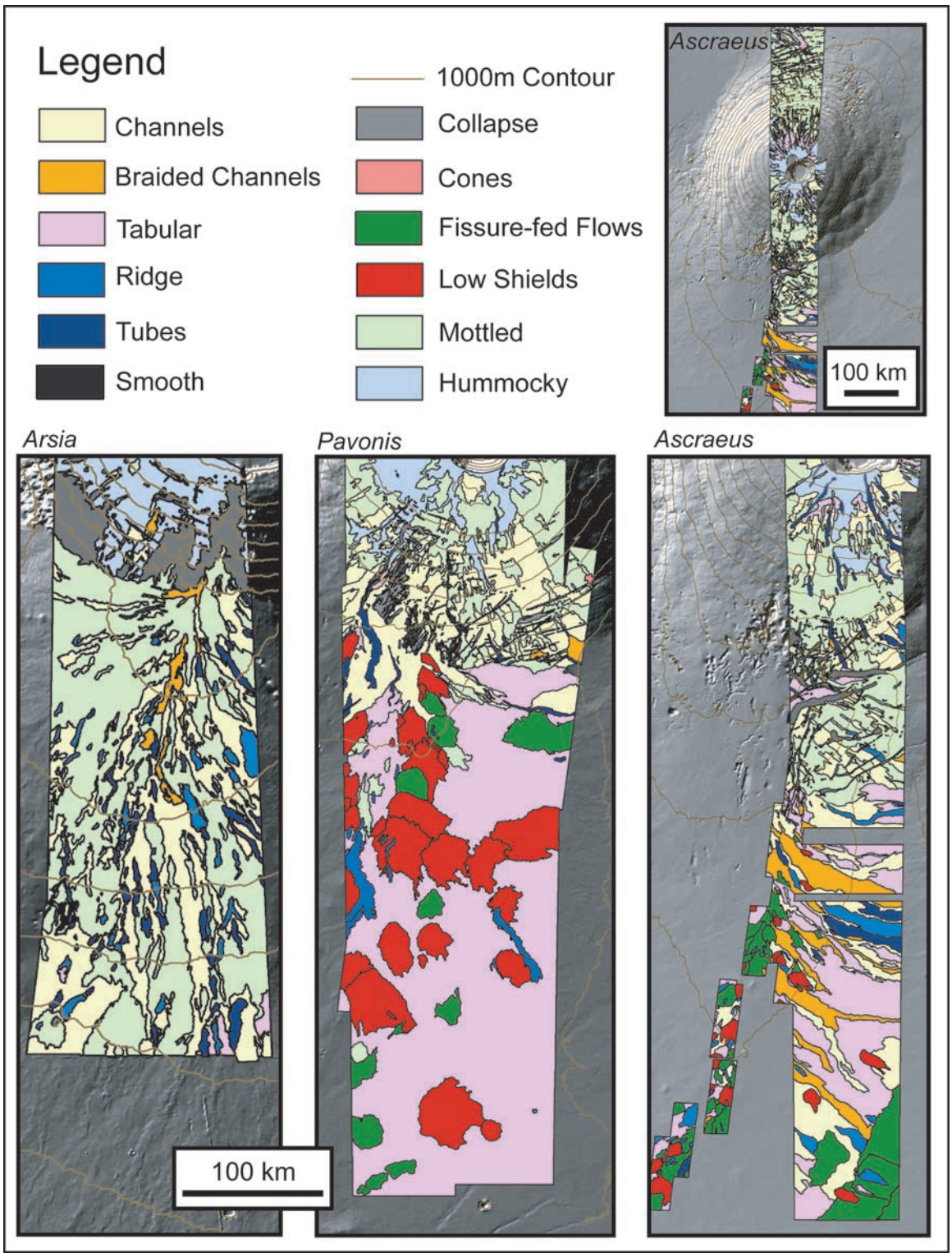

Figure 1. HRSC- and THEMIS-based volcanic unit maps produced in this study showing detail of the southern main flank, rift aprons, and small-vent fields (where present) of the Tharsis Montes. (left) Arsia Mons. (middle) Pavonis Mons. (right) Ascraeus Mons. Map units discussed in the text correspond to colored units in the map legend. A context image showing the entire THEMIS- and HRSC-based map co-registered to MOLA data for Ascraeus Mons is given at the top right.

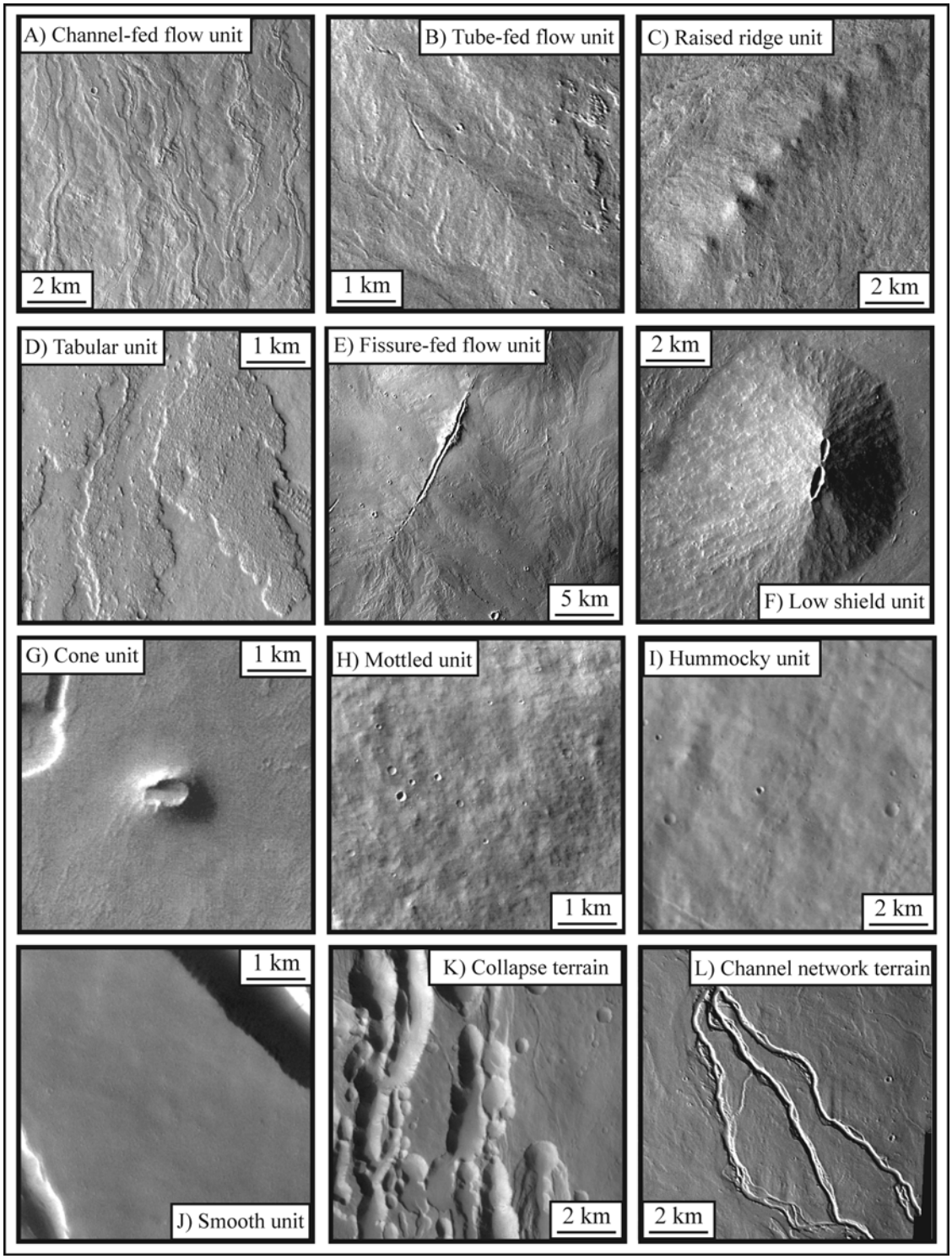

Figure 2. Type examples of ten primary units and two terrains mapped in the Tharsis Montes, using HRSC and THEMIS data. From left to right, top to bottom with image number listed: (a) channel-fed flow unit (H1904), (b) tube-fed flow unit (H0064), (c) raised ridge unit (H1904), (d) tabular unit (V15919004), (e) fissure-fed flow unit (V19312022), (f) low shield unit (V13172008), (g) cone unit (H0891), (h) mottled unit (H0891), (i) hummocky unit (H1904), (j) smooth unit (H1904), (k) collapse terrain (H1904), and (l) channel network terrain (V08155020).

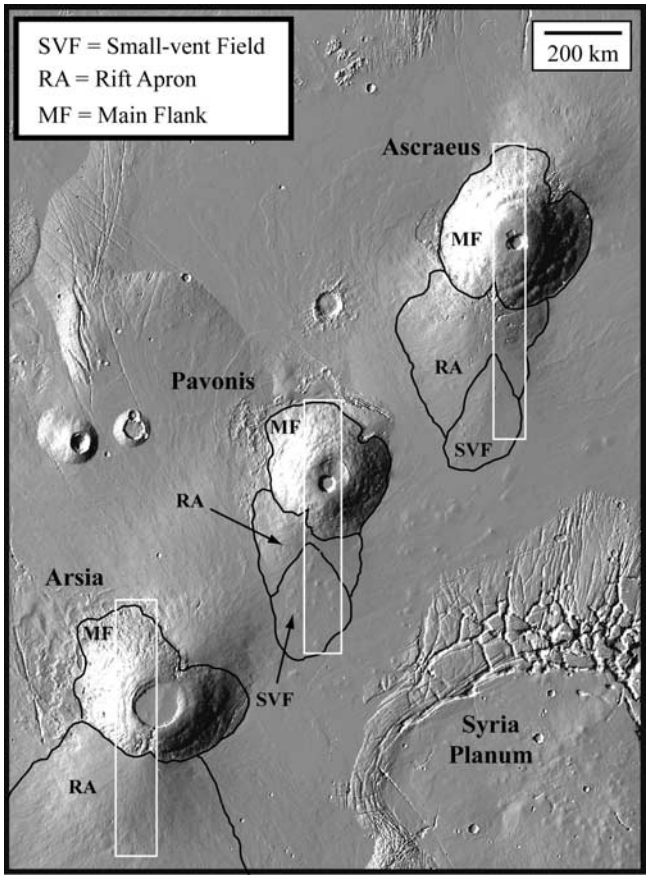

Figure 3. A MOLA shaded relief image showing the Tharsis Montes and the northern half of Syria Planum. The three zones (main flanks, rift aprons, and small-vent fields) discussed in the text are outlined for each shield, and the boundaries of each shield's corresponding HRSC coverage is shown in white. Although rift aprons are also located to the northeast of each shield [*Crumpler and Aubele*, 1978], our maps do not cover those regions and are therefore not shown in the figure. Map zone boundaries are inferred from a combination of mapping conducted in this project and past geologic maps.

assessment of possible volume differences between the shields and of relationships between the lava flows and topography. The median slope was determined for each shield as a measure of its regional slope (all slope values presented within this report are derived from MOLA data), as the median has been shown to best describe the typical slope of a landscape [*Kreslavsky and Head*, 1999, 2000; J. E. Bleacher and R. Greeley, Relating volcano morphology to the developmental progression of Hawaiian shield volcanoes through slope frequency and hypsometric analyses of SRTM data, submitted to *Journal of Geophysical Research*, 2007 (hereinafter referred to as Bleacher and Greeley, submitted manuscript, 2007)].

[10] To determine unit abundances we normalized each unit's surface area to the total map area, enabling a comparison of the abundance of each unit among the Tharsis Montes. We used superposition relationships to provide insight into the sequence of unit emplacement and possible evolution in eruptive style. We synthesized the distribution of flow types among the volcanoes, their relationship to topography, and relative ages to identify trends that might be related to the possible evolution of each volcano. We compare our results for the Tharsis Montes to similar work for the Hawaiian shields to identify any comparable trends that might provide insight into magma production and tectonic setting within the Tharsis province.

4. Results

4.1. Unit Descriptions

[11] We divide the lava flow maps into three zones (Figure 3), including the (1) main flanks, (2) rift aprons (symmetric apron of *Plescia* [2004]), and (3) small-vent fields (linear apron of *Plescia* [2004]), of which the rift apron and small-vent fields are comparable to the satellitic shields described by *Crumpler and Aubele* [1978]. Each zone is composed of a combination of 10 primary map units, of which several were modified producing an additional 2 terrains. These units were defined and characterized using the mapping approach outlined above (Figure 2), including the (1) channel-fed flow unit, (2) tube-fed flow unit, (3) raised ridge unit, (4) tabular unit, (5) fissure-fed flow unit, (6) low shield unit, (7) cone unit, (8) mottled unit, (9) hummocky unit, (10) smooth unit, (11) a collapse terrain, and (12) a channel network terrain. The caldera floors of each shield were omitted from this study. The channel-fed flow, tube-fed flow, raised ridge, tabular, mottled, hummocky, and smooth units as well as the collapse terrain are similar to the units of the same name that were mapped on Olympus Mons [*Bleacher et al.*, 2007], for which the channel- and tube-fed flow units are also described by *Basilevskaya et al.* [2006] and *Pupysheva et al.* [2006].

[12] The channel-fed flow unit is typified by sub-parallel linear channels often displaying levees (Figure 2a). This unit is inferred to be composed of individual channel-fed lava flows, which in many cases overlap to form channel-fed flow fields as are often observed on terrestrial shield volcanoes. The tube-fed flow unit (Figure 2b) is identified by the presence of sinuous chains of collapse pits inferred here to be skylights (e.g., a partially collapsed lava tube roof), which are gradational with sinuous trenches (e.g., a completely collapsed lava tube roof), as is seen on Earth. These structures are often axial to a raised ridge, but also occur within relatively flat terrain. The tube-fed flow unit includes smooth to mottled surfaces adjacent to the collapses, encompassing the ridges where present, and is inferred to represent individual lava tubes and associated lava tube-fed flow fields. The raised ridge unit is similar to the tube-fed flow unit (Figure 2c), but lacks collapses. This unit consists of a sinuous to linear ridge, or a generally linear grouping of topographic mounds, and is inferred to represent inflated tumuli [*Glaze et al.*, 2005] or chains of rootless vents [*Bleacher*, 2007] associated with a lava tube. The tabular unit (Figure 2d) shows relatively smooth surfaces bound by lobate margins. This unit is inferred as the distal margins of channel- or tube-fed flows that cannot be linked to the channel- or tube-fed flow unit, or lava flows emplaced as sheets.

[13] The fissure-fed flow unit (also described by *Mouginis-Mark and Christensen* [2005]) displays a linear trench

generally a few to tens of km long (Figure 2e). Trenches are associated with a topographic rise, in some cases showing rims up to 100 m in height that are likely composed of spatter or cinders, and are inferred to represent linear eruptive vents. The low shield unit is typified by a rise with a central peak (Figure 2f) up to 35 km across and 100 to 200 m high. This unit is inferred to represent low profile, eruptive point sources, or low shields, as described for the Eastern Snake River Plain by *Greeley* [1977b, 1982], which display aspect ratios (height-to-width) roughly an order of magnitude less (~0.01) than those of the Hawaiian shields (~0.20). Included in the low shield and fissure-fed flow units are channel-, tube-, and tabular/sheet-fed flows, which built each edifice. The margins of both units are estimates based on the morphology of lava flows and on MOLA topographic boundaries as was discussed by *Sakimoto et al.* [2003]. However, the boundaries shown in this work might not represent the true extent of lavas erupted from the associated vent area as earlier, possibly more voluminous and longer flows might have been covered by shorter, lower-volume flows erupted from the same source, the latter of which essentially produced the topographic cap of each vent. The cone unit, also typified by a topographic rise with a central peak, is on the order of one kilometer across. Although these features are too small to calculate slope values from MOLA data, they appear to display steeper slopes than the low shield unit (Figure 2g). This unit is inferred to represent cinder or spatter cones for which no associated lava flow fields were identified.

[14] The mottled unit (Figure 2h) is typified by a rough surface at a horizontal scale of tens to hundreds of meters displaying mounds inferred to be only a few meters high on the basis of MOC image analysis. Inferred to be of similar vertical scale to the mottled unit is the hummocky unit, displaying a smooth surface with broad undulations at the horizontal scale of a few kilometers (Figure 2i). Both the mottled and hummocky units lack clear margins, and are often gradational with other units. Whereas the mottled and hummocky units show hilly surfaces at different horizontal scales, the smooth unit lacks flow margins and any clear surface texture (Figure 2j).

[15] Several of the units identified in this project were heavily modified, creating two additional terrains. The collapse terrain (Figure 2k) is typified by chains of ovoid depressions that in some cases form smooth-floored trenches. These features generally display no raised rims, and therefore are considered to represent collapse, rather than impact structures. The channel network terrain, also discussed by *Mouginis-Mark and Christensen* [2005], is composed of channels similar to the channel-fed flow unit in scale, but lack distinct levees while forming branching networks of varied depths (Figure 2l). This terrain tends to originate from fissures and has less easily defined margins than the channel-fed flow unit.

4.2. Unit Abundances and Relationships

[16] Within our map areas all three zones, the main flank, rift apron, and small-vent field (Figure 3), are present at Ascraeus and Pavonis, but no small-vent field was identified at Arsia. The main flanks are dominated by the hummocky and mottled units, which cover between 60 and 70% of the mapped surface at Ascraeus and Pavonis, and ~50% of the mapped surface at Arsia. Nearly 45% of the mapped Arsia main flank is composed of the collapse terrain. The main flanks of the Tharsis Montes display tube- and channel-fed flow unit abundances of 1% and 4% (Arsia), 2% and 16% (Pavonis), and 5% and 21% (Ascraeus), respectively. When in contact, tube-fed flow fields on the main flanks are typically buried by younger channel-fed flow fields. The only identified cones in this study are located on the main flank of Pavonis near the apex of the southwest rift zone. The median slopes of the Tharsis Montes main flanks are 4.3° (Arsia), 3.8° (Pavonis), and 4.6° (Ascraeus), respectively.

[17] Lava flows within the mapped areas of the rift aprons appear to originate within and trend away from large alcoves that are located along the main flank/rift apron boundary (the satellitic calderas of *Crumpler and Aubele* [1978]). Where in contact, rift apron lava flows embay the distal main flanks of each shield. No obvious vent structures are observed within the southwest alcoves (except for the Pavonis cones, which do not appear to have produced lava flow fields). As noted by *Plescia* [2004], the aprons trend S21°W (Arsia), S31°W (Pavonis), and S25°W (Ascraeus), roughly parallel to the trend of the Tharsis Montes. The maximum elevation of lava flows within the rift aprons (as determined from MOLA data) decreases to the northeast from ~12.5 km (Arsia), to ~9.3 km (Pavonis), to ~8.5 km (Ascraeus). In general, lava flows within the rift aprons appear crisper, with more easily identifiable flow margins, than their counterparts within the main flanks. Both the tube- and channel-fed flow units are more abundant within the rift aprons than within the main flanks, comprising 9% and 39% (Arsia), 12% and 47% (Pavonis), and 16% and 31% (Ascraeus) of the mapped rift aprons, respectively. The remaining surface area is composed of the mottled unit and rarely (<4%) the tabular unit. In the rift aprons, tube-fed flows are not consistently embayed by channel-fed flows. The median slopes of the Tharsis Montes southwest rift aprons are 0.8° (Arsia), and 1.0° (Pavonis, Ascraeus), with slopes increasing slightly toward the apron apex as noted by *Mouginis-Mark* [2003].

[18] Generally superposed over the southeastern portions of the Pavonis and Ascraeus rift aprons are small-vent fields. Each plains-style [*Greeley*, 1977b, 1982] volcanic field is composed of at least 30 low shield and fissure vents. Lava flows between the low shields and fissures were emplaced via a combination of lava tubes and extensive sheets, which we assume to have been erupted from the low shields and fissures. These intravent flows coalesce with the vent structures maintaining median slopes of 0.4° (Pavonis) and 0.3° (Ascraeus). Low shields within the Pavonis map comprise two prominent lineaments with trends that transition from S5°W to S15°W distally from the main flank. The axis of the Ascraeus small-vent field is composed of a lineament of low shields and fissures that show a similar change in orientation from S5°W to S20°W.

[19] Except for several channel-fed flow fields on Ascraeus [*Hiesinger et al.*, 2005, 2007] and Arsia, which are truncated by the caldera, the proximal regions of the lava flow fields are buried by younger flows or merge with the hummocky and mottled units. Superposition relationships between flows within the main flanks and rift aprons suggest that distal flows are older than proximal flows, in agreement with previous mapping [*Scott and Tanaka*,

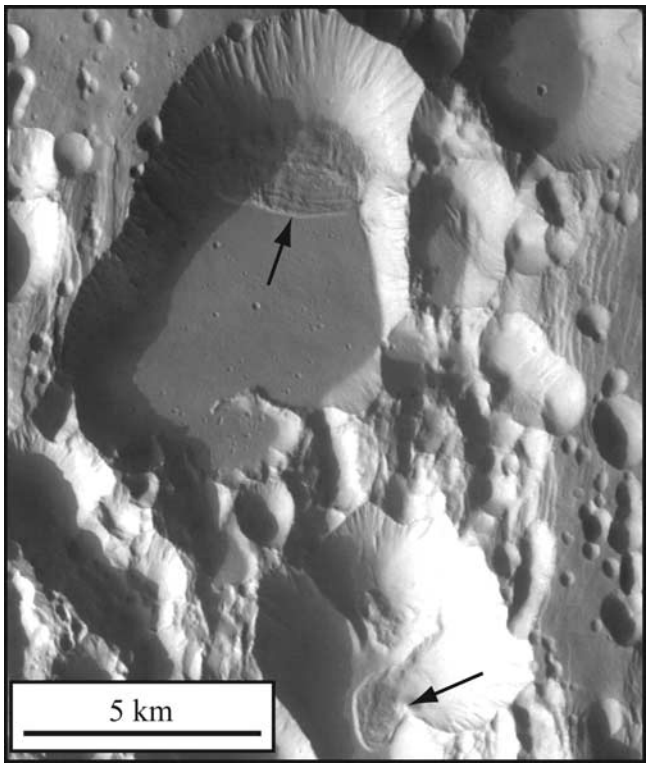

Figure 4. HRSC image H1904 showing two mass movements (arrows) within the Arsia southwest rift alcoves. North is to the top, and illumination is from the bottom left.

1981a, 1981b; *Scott et al.*, 1981a, 1981b, 1981c, 1998; *Scott and Tanaka*, 1986; *Scott and Zimbelman*, 1995]. Within the Pavonis small-vent field, flows associated with low shields tend to embay fissure-fed flow fields, but there is no clear trend in age determined from embayment relationships between the flows of the low shields themselves. Although the small-vent fields are generally superposed on the rift aprons, some younger flows within the rift aprons drape onto the small-vent fields' northern and western margins.

[20] Volumes for the Tharsis Montes, and the parts comprising them, were derived from MOLA data and are comparable to the previously published values of $\sim 10^{15}$ m^3 [*Smith et al.*, 1999; *Wilson et al.*, 2001; *Plescia*, 2004]. The southwest rift apron of Arsia has an estimated volume of $\sim 7 \times 10^{14}$ m^3. The rift aprons, including the small-vent fields, of Pavonis and Ascraeus are nearly an order of magnitude less voluminous at $\sim 9 \times 10^{13}$ m^3.

5. Discussion

5.1. Unit Origins

[21] The channel-fed, tube-fed, raised ridge and tabular units are inferred to be composed of lava flows and flow fields. Within the main flanks these flows appear to have originated from, or near the summit as no other vent structures were found in this study. The low shield, fissure-fed flow, and cone units are inferred to be volcanic vents, and when present, their associated lava flows. Cones are only present within the Pavonis main flank, and do not appear to be related to lava flows. The low shield and fissure-fed flow units appear to have been the source vents for channel-, tube-, and sheet-fed flows. These units are composed of flows that trend directly toward the vent, for which their distal margins are often closely related to a break in slope between the vent's flank and the adjacent intravent flow fields. However, we suggest that the flows comprising each mapped vent, and the intravent flow fields which they embay, were all erupted from the low shields and fissures. This superposition relationship suggests that these vents generally experienced a decrease in flow length with time and that any width or volume calculations should be conducted with caution. Whereas the channel-fed flow unit is the dominant flow unit within the main flanks and rift aprons, the tabular unit is most abundant in the small-vent fields where the median slope is <1°. The low slope in this region likely had an influence on the development of sheet- over channel-fed flows.

[22] The mottled unit covers significant portions of the main flanks and rift aprons. This unit is often transitional with both the channel- and tube-fed flow units, and its surface texture is similar to the surface that comprises the raised ridge and tube-fed flow units. On the basis of these similarities, we suggest that the mottled unit might in part represent tube-fed flow fields for which neither skylights nor ridges are detectable. However, in some cases, MOC images show that the mottled unit is composed of lava channels that are smaller than the detection limit of HRSC and THEMIS, and/or lava channels showing a significant aeolian dust and/or volcanic ash cover.

[23] The Tharsis Montes main flanks are dominated by the hummocky unit, as is the summit of Olympus Mons [*Bleacher et al.*, 2007]. The relatively smooth surface might result in part from caldera spillover lacking in channels and tubes, similar to that seen at Kilauea [*Holcomb*, 1987]. However, thermal inertia values derived from both the Thermal Emission Spectrometer (TES) and THEMIS infrared data suggest that this region is covered by a mantle of dust-sized particles [*Bandfield et al.*, 2000; *Mellon et al.*, 2000; *Ruff and Christensen*, 2002; *Fergason et al.*, 2006; *Nowicki and Christensen*, 2007]. The possible presence of pyroclastic (as previously suggested for the Tharsis province [*Edgett*, 1997; *Edgett et al.*, 1997; *Mouginis-Mark*, 2002]) and/or aeolian deposits could partly mask the presence of underlying lava flow structures, producing a relatively smooth surface.

[24] The Arsia main flank includes large areas of the collapse unit, which is similar to the chaos depressions described by *Basilevsky et al.* [2005] on the western margin of Olympus Mons. They attribute chaos depression formation to collapse resulting from melting of ice deposits held in volatile-rich, dust and pyroclastic layers that in some places produce a smooth surface. Furthermore, at lower elevations on the western Arsia flank, outside of our map area, extensive volatile-rich deposits are suggested to have accumulated in the Amazonian [*Head and Marchant*, 2003; *Shean et al.*, 2007]. Mass movements within the Arsia alcoves (Figure 4), which are lacking at the other Tharsis Montes, might have formed more easily here due to the presence of weakly consolidated layers interbedded with the lava flows. The possible presence of friable deposits contributing to alcove wall collapse, a similar relationship between the hummocky unit and collapses at Arsia and

Table 1. Trends That Exist Across the Tharsis Montes Rift Aprons[a]

	Arsia Mons	Pavonis Mons	Ascraeus Mons
Median slope, deg	0.8	1.0	1.0
Percent surface area covered by tube-fed flow unit	9	12	16
Channel- to tube-fed flow unit ratios	4.3	3.8	2.0
Rift apron volumes, m^3	$\sim 7 \times 10^{14}$	$\sim 9 \times 10^{13}$	$\sim 9 \times 10^{13}$
Maximum elevation of flows within the rift aprons, km	12.5	9.3	8.5

[a]Median slope and abundance of the tube-fed flow unit increase from Arsia to Ascraeus, while the channel- versus tube-fed flow unit ratios, rift apron volumes, and the maximum elevation at which flows within the rift aprons were identified all increase across the chain.

Olympus Mons [*Basilevsky et al.*, 2005], and the inferred accumulation of ices adjacent to our map area [*Head and Marchant*, 2003; *Shean et al.*, 2007] leads us to suggest that the hummocky unit likely resulted from the accumulation of frozen volatiles, aeolian dust, and/or volcanic ash, which produced a broad, smooth unit with slight topographic undulations (at the horizontal scale of kilometers) that overlies the pre-existing Arsia main flank lava flows.

[25] The channel network terrain appears to have formed as a result of erosion. Similar structures are previously suggested to have been eroded by liquid volatiles [*Carr*, 1981, 1996; *Baker*, 1982; *Mouginis-Mark*, 1985, 1990; *Scott and Wilson*, 1998, 1999; *Burr et al.*, 2002; *Head et al.*, 2003; *Mouginis-Mark and Christensen*, 2005; *Fassett and Head*, 2006], and fluid lavas [*Wilson and Mouginis-Mark*, 1984, 2001; *Leverington*, 2004; *Williams et al.*, 2005]. The channel network terrain commonly originates along fissures, which could be the source region for either erosive material. Continued mapping of the channel network terrain with higher resolution images should provide insight into its origin.

5.2. Trends

[26] Within the main flank zones in our mapped areas, most of the channel- and tube-fed flow units are embayed by the hummocky unit where they are in contact. Less common are younger lava channels that overlie the hummocky unit and are truncated by the caldera in their proximal region. Although some tube-fed flows embay older channel-fed flows, there are no examples of tube-fed flows that are entirely unembayed by channel-fed flows, suggesting that the surface flows record a complex emplacement history, but that in general a transition from tube- and channel- to strictly channel-forming eruption conditions occurred. A similar transition is suggested to have occurred at Olympus Mons [*Bleacher et al.*, 2007], and *Cattermole* [1987, 1990], *Schneeberger and Pieri* [1991], and *Ivanov and Head* [2006] have identified changes in late-stage eruptive dynamics at Alba Patera. The ratio of the channel- to tube-fed flow units range from 4:1 (Arsia and Ascraeus) to 8:1 at Pavonis. The collapse terrain cuts all other units on the main flanks of the Tharsis Montes.

[27] The rift aprons were previously recognized to embay the main flanks [*Carr et al.*, 1977; *Crumpler and Aubele*, 1978; *Greeley and Spudis*, 1981]. Our mapping confirms that no lava flows from the main flanks embay lava flows of the rift aprons [*Crumpler and Aubele*, 1978], nor do they drape into the collapse terrain. Within the rift aprons several trends were identified across the Tharsis Montes chain (Table 1). The maximum elevation of rift apron units decreases from 12.5, to 9.3, to 8.5 km (Arsia to Ascraeus respectively), and the estimated apron volume decreases from $\sim 7 \times 10^{14}$ m^3 to $\sim 9 \times 10^{13}$ m^3. Median slope increases slightly from 0.8° at Arsia to 1.0° at Pavonis and Ascraeus. The abundance of the tube-fed flow unit increases from 9%, to 12%, to 16%, while the channel- to tube-fed flow unit ratios decrease from 4.3, to 3.8, to 2.0 from Arsia to Ascraeus, respectively. Most tube-fed flows in the Arsia rift apron are embayed by younger channel-fed flows. However, unembayed tube-fed flows are common within the Pavonis and Ascraeus rift aprons.

[28] The development of the small-vent fields appears to be the most recent effusive event. Arsia lacks a small-vent field associated with its southwest rift apron, but does contain a chain of low shields superposed on its late Amazonian–aged caldera floor [*Carr et al.*, 1977; *Crumpler and Aubele*, 1978; *Mouginis-Mark*, 2003]. The Pavonis small-vent field is generally superposed over the southeast portion of the rift apron. Several channel-fed flows from the rift apron drape over the small-vent field, but most are truncated by flows of the small-vent field. This superposition relationship attests to the coeval development of the two zones, although the majority of Pavonis flows comprising the small-vent field are younger than the flows of the rift apron. The Ascraeus small-vent field displays a less clear superposition relationship with the adjacent rift apron. Within our map area, the closest vent structures are nearly 120 km from the main flank extending out to at least 430 km, and the apron axes display the highest density of vents within the respective rift aprons.

5.3. Sequential History

[29] The previously established developmental sequence for the Tharsis Montes [*Crumpler and Aubele*, 1978] includes main edifice construction through eruption of basaltic lavas at the summit, followed by eruptions along linear vents (rift zones) on the northeast and southwest portions of the main flanks [*Carr*, 1973; *Greeley*, 1973; *Carr et al.*, 1977; *Greeley and Spudis*, 1981]. Crater counts [*Plescia and Saunders*, 1979; *Neukum and Hiller*, 1981; *Werner*, 2005] support the suggestion by *Crumpler and Aubele* [1978] that the last stage of the developmental sequence involved resurfacing in the late Amazonian. Although we cannot determine the depth of deposits or total volume of erupted material during the late Amazonian eruptive sequence, our mapping over ~20% of each shield is used to infer new insight into the eruptive dynamics at the Tharsis Montes during this time period.

[30] *Crumpler and Aubele* [1978] state that while main flank construction and parasitic shield (hereafter referred to as rift apron) development might have occurred concurrently, rift apron development likely postdates major shield building. However, the amount of time, if any, that passed between these two major Tharsis Montes events remains

in question. Our mapping shows a consistent embayment of main flank lava flows by rift apron flows as seen by *Crumpler and Aubele* [1978]. Furthermore, we identified no instances of embayment of the collapse terrain by main flank lava flows; whereas embayment relationships suggest that rift apron lava flows were emplaced synonymously with collapse terrain formation. These superposition relationships suggest that main flank development, at least in the distal margins, was complete before collapse terrain formation and rift apron eruptions began, supporting *Crumpler and Aubele*'s [1978] conclusions.

[31] Recent tectonic mapping of the Tharsis Montes [*Byrne et al.*, 2007] show that previously recognized terraces [*Carr et al.*, 1977] are potentially more extensive than originally thought on the main flanks, but are not present within the rift aprons. Although the mechanisms responsible for the formation of these features are currently a source of debate [*Carr et al.*, 1977; *Thomas et al.*, 1990; *McGovern and Solomon*, 1993; *Morgan and McGovern*, 2005], they are thought to be slow acting. *Byrne et al.* [2007] note that whatever the mechanism(s) of formation for flank terraces, they must have occurred late in the volcano's development, or occurred repeatedly throughout its construction so as not to be buried by younger volcanic deposits. On the basis of our mapped superposition relationships, and because slow forming terraces are present on the main flank, but never formed within or were completely buried by younger rift apron flows, we suggest that the transition from main flank to rift apron development was associated with an eruptive hiatus at each of the Tharsis Montes.

[32] Main flank superposition relationships also indicate that through time, shorter lava flows, and higher abundances of channel-fed flows relative to tube-fed flows were emplaced, followed by the emplacement of the hummocky unit, and later by the emplacement of less extensive channel-fed flows from the summit. The origin of the hummocky unit is important for understanding the recent eruptive history. If it is composed of volatiles and aeolian dust, then late Amazonian main flank resurfacing was dominated by aeolian processes following emplacement of the majority of main flank flows. In contrast, if caldera overflow and/or volcanic ash deposition formed the hummocky unit then it represents a stage of the main flank eruptive sequence between the emplacement of the bulk of main flank lava flows and the more recent emplacement of less extensive lava channels. Continued mapping of the Tharsis Montes as well as analysis of higher resolution data, such as those currently returning from the HiRISE camera [*McEwen et al.*, 2007] might better reveal the nature of this unit.

[33] The rift aprons appear to be the source region for some of the longest traceable channel-fed flows on Mars [*Zimbelman*, 1985, 1998; *Baloga et al.*, 2003; *Glaze and Baloga*, 2006; *Garry et al.*, 2007]. However, superposition relationships indicate that flow lengths decreased with time as is seen on the main flanks, and on Hawaiian volcanoes. Unlike the main flanks, the rift aprons do not show a consistent embayment relationship between the channel- and tube-fed flow units. The Arsia southwest rift apron is more voluminous than the other Tharsis Montes rift aprons, and is associated with the development of a linear group of low shields across the caldera floor [*Carr et al.*, 1977; *Crumpler and Aubele*, 1978; *Mouginis-Mark*, 2003]. Pavonis and Ascraeus do not display rift-related eruptive vents at their summits, but developed fields of low shields, fissures, and associated flow fields. On the basis of the superposition relationships between the two zones at Pavonis and Ascraeus, it appears that the small-vent fields formed synonymously with the end of rift apron eruptions at each volcano.

[34] The late Amazonian eruptive sequence for the Tharsis Montes, derived here from a combination of lava flow and tectonic mapping, and comparison with the trends seen at the Hawaiian volcanoes, comprise (1) eruptions within the main flanks, including emplacement of channel- and tube-fed flows from the main flank summit, transitioning to dominantly channel-fed flows of decreasing length, transitioning to or followed by emplacement of the hummocky unit, and later less extensive channel-fed flows that embay the hummocky unit, (2) eruptions within the rift aprons, including formation of the collapse terrain synonymously with emplacement of channel- and tube-fed flows within the rift aprons, while lava flows appear to have decreased in length with time within each zone, and (3) development of fields of small eruptive vents up to several hundred kilometers from the main flanks at Ascraeus and Pavonis, and within the summit caldera at Arsia, both coevally and subsequent to the emplacement of lava flows within the rift aprons.

[35] The trends across the Tharsis Montes (Table 1) are similar to several trends seen among the Hawaiian shield volcanoes where long-lived, voluminous eruptions of tholeiitic lavas, physically buffered from below the magma chamber, produce more tube-fed flows in the early stages of shield development while experiencing the highest magma production rates. A transition to shorter-lived, unbuffered eruptions of alkalic lavas associated with decreased magma production rates due to plate motion causes an increase in lava channel development and increased flank slopes [*Greeley*, 1987; *Holcomb*, 1987; *Lockwood and Lipman*, 1987; *Moore and Mark*, 1992; *Rowland and Garbeil*, 2000; Bleacher and Greeley, submitted manuscript, 2007]. In the later stages of development, continued decrease in magma production results in smaller, isolated bodies of magma, some of which ascend to the surface resulting in the late stage development of small, parasitic eruption vents [*Wolfe et al.*, 1997]. Comparison to the Hawaiian shields, an age-progressive chain of shield volcanoes linked to a common magma source, suggests that the late Amazonian eruptive sequence at the Tharsis Montes might have resulted from a common magma source that shows a decrease in magma production through time.

6. Implications

[36] The Tharsis Montes are located northwest of the topographic center of the Tharsis province [*Smith et al.*, 1999], a volcanic rise that spans 4,500 km across the western hemisphere of Mars. The province includes an array of volcanic features including seven partly buried shield volcanoes, lava plains including clusters of low shields and fissure vents [*Mouginis-Mark et al.*, 1992; *Hodges and Moore*, 1994], and a wide variety of tectonic features, including radial grabens, and circumferential wrinkle ridges [*Tanaka et al.*, 1991; *Banerdt et al.*, 1992], with ages spanning much of

the history of the planet. Detailed mapping of the tectonic features led *Anderson et al.* [2001] to determine that the structures formed during at least five major episodes throughout the history of the Tharsis province, decreasing in intensity through time [*Plescia and Saunders*, 1982; *Mège and Masson*, 1996; *Wilson and Head*, 2002]. *Anderson et al.* [2001, 2004] suggest that each episode represents a broad magmatic-driven tectonic event, associated with a large mantle upwelling, the emplacement of radial dikes and fractures, extensive lava flow fields, and small-vent fields.

[37] *Carr* [1974] noted that the observed tectonic features radial to the Tharsis Montes do not match the expected pattern if each shield is considered as an independent source of regional stress. However, subsequent mapping showed that late Amazonian features match well with a single tectonic center under the Tharsis Montes chain [*Plescia and Saunders*, 1982; *Mège and Masson*, 1996; *Anderson et al.*, 2001; *Wilson and Head*, 2002]. Our lava flow mapping has revealed several trends across the Tharsis Montes that when compared to the Hawaiian volcanoes also suggest that eruptions at all three volcanoes might be linked to a single source. If the event responsible for the development of late Amazonian tectonic features radial to the Tharsis Montes is the result of a single magmatic upwelling, then the late Amazonian eruptive sequence described above for the Tharsis Montes should also be linked to this single potential magma source.

[38] The following discussion includes only the late Amazonian sequence at the Tharsis Montes, which themselves are thought to be much older [*Plescia and Saunders*, 1979; *Neukum and Hiller*, 1981, *Neukum et al.*, 2004b; *Werner*, 2005]. As such we assume that the main flanks of each volcano, and possibly the rift zones, developed prior to emplacement of the late Amazonian lava flows. If these eruptions are linked to one magma source, then the morphologic trends listed in Table 1 are likely related to the order of magma delivery to each volcano relative to the lifespan of the upwelling (Figure 5). Ascending magma produced above a large magmatic upwelling beneath the Tharsis Montes might have preferentially followed previously established, permanent low-viscosity zones associated with each shield, as are suggested to exist by *Wilson et al.* [2001] as a result of episodic magma rise throughout the development of each shield. If the upwelling originated near Arsia, the largest volume of magma would likely be delivered there first (Figure 5a). Some amount of magma reached the summit, possibly emplacing channel-fed flow fields over the hummocky unit and resurfacing the caldera floors. However, these flows did not reach the distal portions of the main flank and are much smaller in length (and presumably volume) than the lava flows that resurfaced the rift aprons during the same time period. Most of the magma appears to have been erupted through the rift zones, thereby resurfacing the rift aprons with a combination of channel- and tube-fed flows for which no clear embayment relationship exists at the two northern shields, as is seen at younger Hawaiian volcanoes.

[39] As the upwelling impinged upon the lithosphere, the melt zone (suggested by *Mège and Masson* [1996] to be on the order of 1000 km in diameter or greater) would likely have spread out (Figure 5b), thereby beginning to deliver magma to Pavonis and later to Ascraeus and potentially producing the trends that we identified in our mapping. Although our results do not support, nor refute, the possibility of plume migration on Mars, the lava flow trends at the Tharsis Montes (which at Hawaii are attributed to a moving plate over a stationary magma source) might also be explained by migration of the magma source underneath a stationary plate (Figure 5c). Terrestrial plumes are thought to be stationary with respect to the faster moving lithospheric plates, but likely move up to several mm/yr [*Courtillot et al.*, 2003]. Therefore the possibility of melt zone movement beneath the crust, which has previously been mentioned as a possibility for Mars [*Anderson*, 1988; *Mège and Masson*, 1996] should at least be considered when attempting to interpret eruptive sequences in the Tharsis province. Whether a result of melt zone spreading, migration, or both, lava flow trends suggest that magma delivery started at Arsia first and subsequently occurred toward the northern shields. As magma delivery progressed to the north, small batches of magma ascended, possibly along preexisting fractures that were produced during previous events (such as the north trending features of Claritas Fossae [*Anderson et al.*, 2001]) or as the last stages of magma ascension at each shield. These smaller batches of magma could have formed small eruptive vents such as the low shields and fissures that together form the small-vent fields [*Hughes et al.*, 2005], which do not parallel the orientation of the Tharsis Montes or the rift aprons.

[40] Similar volcanic deposits, including extensive channel-, tube-, and sheet-fed flow fields, and clusters of small vents, as well as radiating tectonic features are also present at Syria Planum [*Hodges and Moore*, 1994; *Sakimoto et al.*, 2003; *Anderson et al.*, 2004; *Schupack and Sakimoto*, 2006; *Baptista et al.*, 2006, 2007], a site also suggested to have experienced a large magmatic upwelling [*Anderson et al.*, 2001, 2004]. The occurrence of similar volcanic and tectonic features at Syria Planum, presumably related to a magmatic upwelling, supports the hypothesis that a similar, shared magma source beneath the Tharsis Montes is responsible for the late Amazonian–aged volcanics and tectonics.

[41] Comparison with the Hawaiian volcanoes shows that as magma production decreases and eruption conditions change at shield volcanoes the abundance of tube-fed flows decreases, resulting in their embayment by younger channel-fed flows. A similar trend is seen at Arsia. However, the younger shields to the north, where magma would have been delivered later, show this relationship less clearly. The lava flow relationships related to volcano age suggest that the development of channel-fed flows did not reach a volume large enough to bury the previously emplaced tube-fed flows, or that the eruptive sequence is not yet complete at the northern Tharsis Montes. As magma production waned at each of the volcanoes the number of eruptive vents increased, producing low shields in the caldera of Arsia [*Crumpler and Aubele*, 1978; *Mouginis-Mark*, 2003] and plains-style [*Greeley*, 1977b, 1982] volcanic fields at greater distances from the main flanks at Pavonis and Ascraeus.

[42] The lava flow mapping conducted in this study is a preliminary analysis of the late Amazonian eruptive sequence for the Tharsis Montes based on one transect for

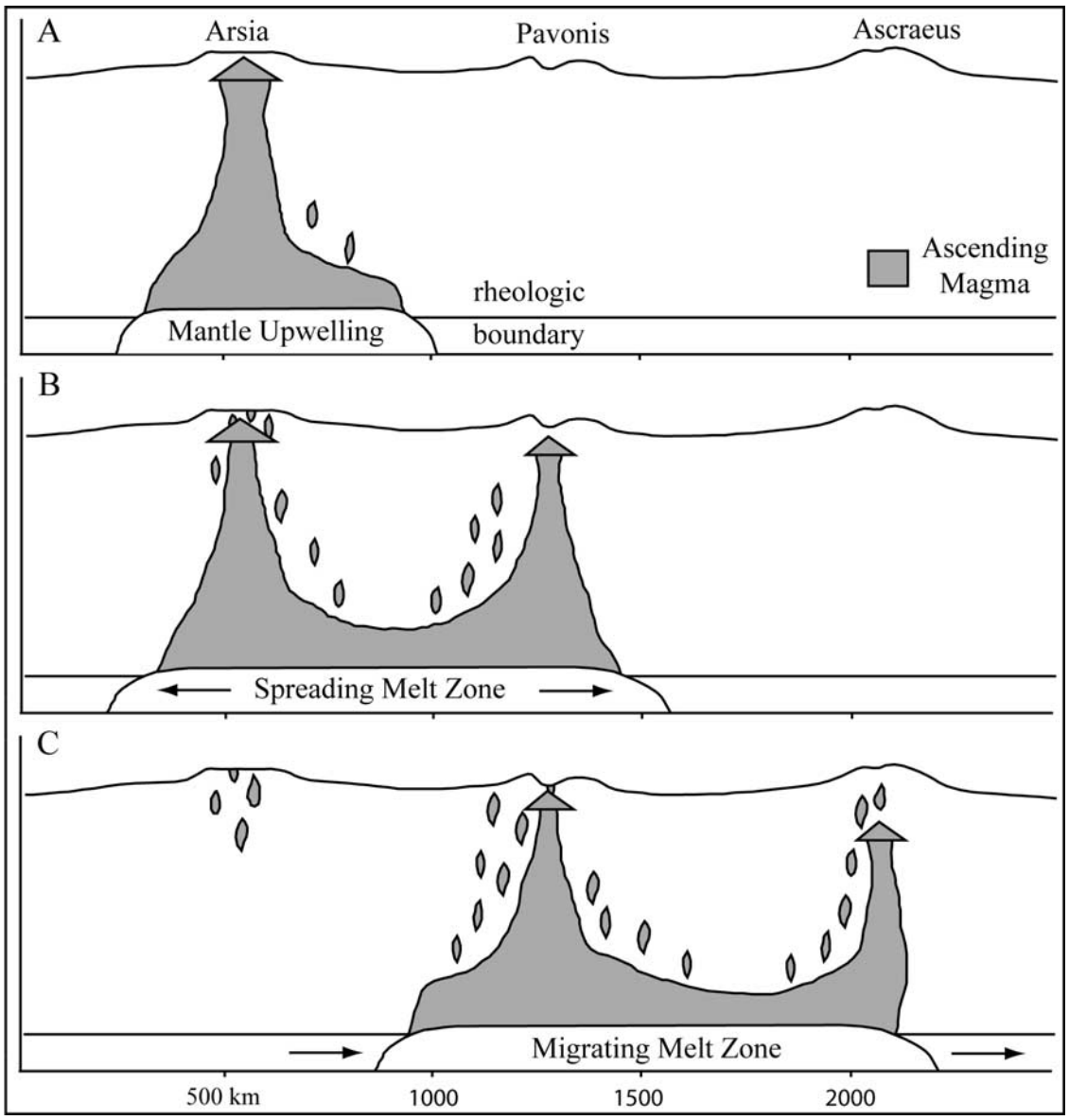

Figure 5. Stylized cross sections derived from MOLA data showing a conceptual large mantle upwelling impinging upon the lithosphere beneath the Tharsis Montes. In this scenario, (a) initial magma delivery occurs at Arsia along an existing, low-viscosity zone beneath the shield, and lavas are erupted through the established rift zones. (b) As the upwelling impinges on the lithosphere, it spreads out and begins to deliver magma to Pavonis. (c) Continued spreading and/or possible migration of the melt zone toward the northeast initiates magma delivery to Ascraeus as the magma supply to Arsia begins to taper off. Small magma bodies might ascend along previously developed crustal fractures or along radial dikes, thereby forming low shields and fissure vents.

each shield that sampled the main flanks, southwest rift aprons, and small-vent fields. *Parfitt et al.* [1993] and *Parfitt and Head* [1993] show that lateral dike emplacement, which is typical of rift zone activity [*Walker*, 1999], is expected during buffered eruptions of basaltic volcanoes. The Tharsis Montes are clearly related to a northeast trending structural pattern [*Carr et al.*, 1977; *Mouginis-Mark et al.*, 1992] that likely also controlled the development of the rift zones. However, while deep structural patterns can control rift zone development [*Walker*, 1999], *Parfitt et al.* [1993] note that lateral migration of dikes might be expected in any direction. Continued mapping is required to assure that the observed trends are not a result of sampling bias. Complete mapping of each shield and its surroundings should show if regional tectonics have restricted the development of rift zones solely to the northeast and southwest flanks, as well as enabling a more accurate understanding of the unit relationships between the hummocky unit and the younger channel-fed flows.

7. Conclusions

[43] The Tharsis Montes each display a main flank dominantly constructed by emplacement of lava flow fields

from summit eruptions, and lava aprons to the southwest and northeast, constructed by emplacement of lava flow fields erupted along northeast-trending rift zones prevalent through all three shields [*Crumpler and Aubele*, 1978]. Lava flow mapping of HRSC, THEMIS, MOC, and MOLA data conducted in this study provide insight into the eruptive history of this volcanic chain. The main flanks show a transition from tube- to channel-forming eruption conditions (which at Hawaii are related to a decrease in magma production), followed by the emplacement of the hummocky unit, which is likely composed of frozen volatiles, dust, and/or pyroclastics, all of which were previously suggested to exist across the Tharsis Montes. The rift aprons show an increase in tube-fed flow abundances, number of eruptive vents, and rift apron slope, and a decrease in the ratios of the channel- to tube-fed flow units, rift apron volume, and maximum elevation of rift apron units, from Arsia through Pavonis to Ascraeus. These trends suggest that the late Amazonian eruptive sequence across the Tharsis Montes possibly resulted from a shared magma source that first delivered magma to Arsia, then Pavonis, and finally Ascraeus, as similar trends are known to exist at the Hawaiian shields due to plate motion over a shared source.

[44] On the basis of comparison with the established tectonic history of the Tharsis province, it appears that the previously constructed Tharsis Montes were located above a late Amazonian magmatic upwelling that occurred synchronously with volcanic resurfacing of the shields. Episodic activity associated with previous Tharsis province upwellings likely established permanent, low-viscosity zones beneath each shield [*Wilson et al.*, 2001], which could have served as the easiest pathway for ascent of magmas derived from the most recent magmatic-tectonic event. Syria Planum, resulting from an older Hesperian convective upwelling, shows development of small-vent fields, extensive lava flow fields, and radiating tectonic features. The same morphologies are shown across the Tharsis Montes, where extensive lava flow fields appear to have transitioned to low shield and fissure development. The primary difference between upwellings at Syria and the Tharsis Montes is the presence of the previously constructed shield volcanoes.

[45] The conceptual model presented here relates our preliminary mapping results, showing late Amazonian trends in effusive activity between the Tharsis Montes, to the presumed magmatic-driven tectonic history of the province during the same time period. Even if the most recent volcanic resurfacing of the Tharsis Montes was not initiated by the large magmatic upwelling responsible for the development of the tectonic features radial to the chain, the overlap in time and space between the most recent tectonic episode and eruptions at these shields suggests that this major Tharsis province event likely influenced to some degree the style of eruption along the Tharsis Montes rift zones in the late Amazonian.

[46] One issue of interest for future work is the mechanism of formation for the extensive rift zones prevalent across the Tharsis Montes chain with regard to the processes responsible for the formation of the main flanks. The shields are clearly related to a northeast trending structural pattern [*Carr et al.*, 1977; *Mouginis-Mark et al.*, 1992] that likely also controlled the development of rift zones. However, it is not clear why the Tharsis Montes transitioned from main shield construction to major rift apron development while other volcanoes, such as Olympus Mons, do not appear to have experienced a similar transition. If late stage volcanism across the Tharsis Montes is related to a single large magmatic upwelling emplaced over previously formed shield volcanoes, then late Amazonian volcanic and tectonic activity in this area could represent a different style of magma production and eruption style than was responsible for main flank formation.

[47] **Acknowledgments.** We thank the HRSC Experiment Teams at DLR Berlin and Freie Universitaet Berlin as well as the Mars Express Project Teams at ESTEC and ESOC for their successful planning and acquisition of data as well as for making the processed data available to the HRSC Team. We acknowledge the effort of the HRSC Co-Investigator Team members and their associates who have contributed to this investigation in the preparatory phase and in scientific discussions within the Team. We appreciate the comments of E. Hauber throughout this project, and we thank T. Gregg and K. Mitchell for their insightful comments and thorough reviews of our manuscript. This work is supported by a NASA GSRP grant to J. E. B. and NASA funding to R. G. as a Co-Investigator on the HRSC experiment on Mars Express.

References

Anderson, R. C. (1988), Lineament analysis and tectonic interpretation for the central Tharsis region, Mars (abstract), *Proc. Lunar Planet. Sci. Conf. 19th*, 12.

Anderson, R. C., J. M. Dohm, M. P. Golombek, A. F. C. Hadermann, B. J. Franklin, K. L. Tanaka, J. Lias, and B. Peer (2001), Primary centers and secondary concentrations of tectonic activity through time in the western hemisphere of Mars, *J. Geophys. Res.*, *106*(E9), 20,563–20,585.

Anderson, R. C., J. M. Dohm, A. F. C. Haldermann, T. M. Hare, and V. R. Baker (2004), Tectonic histories between Alba Patera and Syria Planum, Mars, *Icarus*, *171*, 31–38.

Bailey, J. E., A. J. L. Harris, J. Dehn, S. Calvari, and S. K. Rowland (2006), The changing morphology of an open lava channel on Mt. Etna, *Bull. Volcanol.*, *68*, 497–515, doi:10.1007/s00445-005-0025-6.

Baker, V. R. (1982), *The Channels of Mars*, 198 pp., Univ. of Tex. Press, Austin.

Baloga, S. M., P. J. Mouginis-Mark, and L. S. Glaze (2003), Rheology of a long lava flow at Pavonis Mons, Mars, *J. Geophys. Res.*, *108*(E7), 5066, doi:10.1029/2002JE001981.

Bandfield, J. L., V. E. Hamilton, and P. R. Christensen (2000), A global view of Martian surface compositions from MGS-TES, *Science*, *287*, 1626–1630.

Banerdt, W. B., M. P. Golombek, and K. L. Tanaka (1992), Stress and tectonics on Mars, in *Mars*, edited by H. H. Kieffer et al., pp. 249–297, Univ. of Ariz. Press, Tucson.

Baptista, A. R., N. Mangold, V. Ansan, E. I. Alves, P. Logonne, and the HRSC and OMEGA Teams (2006), The unique volcanic type of Syria Planum, Mars: Geophysical analysis using Mars Express–HRSC and OMEGA data, Abstract EPSC2006-A-00213 presented at European Planetary Science Congress, Eur. Planet. Network, Berlin, 18–22 Sept.

Baptista, A. R., N. Mangold, V. Ansan, E. I. Alves, P. Logonne, and the HRSC and OMEGA Teams (2007), A swarm of small shield volcanoes on Syria Planum, Mars, analyzed using Mars Express–HRSC data, Abstract EDU2007-A-08342 presented at EGU General Assembly, Eur. Geosci. Union, Vienna.

Basilevskaya, E. A., G. Neukum, and the HRSC Co-Investigator Team (2006), The Olympus volcano on Mars: Geometry and characteristics of lava flows, *Sol. Syst. Res.*, *40*(5), 375–383.

Basilevsky, A. T., et al. (2005), Morphology and geological structure of the western part of the Olympus Mons volcano on Mars from analysis of the *Mars Express* HRSC Imagery, *Sol. Syst. Res.*, *39*, 85–101.

Bleacher, J. E. (2007), Observations of the Campout tube-fed flow encountering a slope break, Kilauea, Hawaii: An analogue to lava fans on Olympus Mons, Mars, *Lunar Planet. Sci.* [CD-ROM] *XXXVIII*, Abstract 1886.

Bleacher, J. E., R. Greeley, D. A. Williams, S. C. Werner, E. Hauber, and G. Neukum (2007), Olympus Mons, Mars: Inferred changes in late Amazonian aged effusive activity from lava flow mapping of Mars Express High Resolution Stereo Camera data, *J. Geophys. Res.*, *112*, E04003, doi:10.1029/2006JE002826.

Burr, D. M., J. A. Grier, A. S. McEwen, and L. P. Keszthelyi (2002), Repeated aqueous flooding from the Cerberus Fossae: Evidence for very recently extant, deep groundwater on Mars, *Icarus*, *159*, 53–73.

Burrough, P. A., and R. A. McDonell (1998), *Principles of Geographical Information Systems*, 2nd ed., 356 pp., Oxford Univ. Press, New York.
Byrne, P. K., J. B. Murray, B. van Wyk de Vries, and V. R. Troll (2007), Flank terrace architecture of Martian shield volcanoes, *Lunar Planet. Sci.* [CD-ROM], *XXXVIII*, Abstract 2380.
Calvari, S., and H. Pinkerton (1998), Formation of lava tubes and extensive flow field during the 1991–1993 eruption of Mount Etna, *J. Geophys. Res.*, *103*(B11), 27,291–27,301.
Calvari, S., and H. Pinkerton (1999), Lava tube morphology on Etna and evidence for lava flow emplacement mechanism, *J. Volcanol. Geotherm. Res.*, *90*, 263–280.
Calvari, S., M. Neri, and H. Pinkerton (2003), Effusion rate estimations during the 1999 summit eruption on Mount Etna, and growth of two distinct lava flow fields, *J. Volcanol. Geotherm. Res.*, *119*, 107–123.
Carr, M. H. (1973), Volcanism on Mars, *J. Geophys. Res.*, *78*, 4049–4062.
Carr, M. H. (1974), Tectonism and volcanism of the Tharsis region of Mars, *J. Geophys. Res.*, *79*, 3943–3949.
Carr, M. H. (1975), Geologic map of the Tharsis Quadrangle of Mars, scale 1:5,000,000, *U.S. Geol. Surv. Misc. Invest. Ser.*, *Map I-0893*.
Carr, M. H. (1981), *The Surface of Mars*, 232 pp., Yale Univ. Press, New Haven, Conn.
Carr, M. H. (1996), *Water on Mars*, 229 pp., Oxford Univ. Press, New York.
Carr, M. H., and R. Greeley (1980), Volcanic features of Hawaii: A basis for comparison with Mars, *NASA Spec. Publ.*, *NASA SP-403*, 211 pp.
Carr, M. H., R. Greeley, K. R. Blasius, J. E. Guest, and J. B. Murray (1977), Some Martian volcanic features as viewed from the Viking orbiters, *J. Geophys. Res.*, *82*, 3985–4015.
Cattermole, P. (1987), Sequence, rheological properties, and effusion rates of volcanic flows at Alba Patera, Mars, *Proc. Lunar Planet. Sci. Conf 17th*, Part 2, *J. Geophys. Res.*, *92*, suppl., E553–E560.
Cattermole, P. (1990), Volcanic flow development at Alba Patera, Mars, *Icarus*, *83*, 453–493.
Christensen, P. R., et al. (2004), The Thermal Emission Imaging System (THEMIS) for the Mars 2001 Odyssey Mission, *Space Science Reviews*, *110*, 85–130.
Courtillot, V., A. Davaille, J. Besse, and J. Stock (2003), Three distinct types of hotspots in the Earth's mantle, *Earth Planet. Sci. Lett.*, *205*, 295–308.
Crumpler, L. S., and J. C. Aubele (1978), Structural evolution of Arsia Mons, Pavonis Mons, and Ascreus Mons: Tharsis region of Mars, *Icarus*, *34*, 496–511.
Edgett, K. S. (1997), Aeolian dunes as evidence for explosive volcanism in the Tharsis region of Mars, *Icarus*, *130*, 96–114.
Edgett, K. S., B. J. Butler, J. R. Zimbelman, and V. E. Hamilton (1997), Geologic context of the Mars radar "Stealth" region in southwestern Tharsis, *J. Geophys. Res.*, *102*(E9), 21,545–21,567.
Fassett, C. I., and J. W. Head (2006), Valleys on Hecates Tholus, Mars: Origin by basal melting of summit snowpack, *Planet. Space Sci.*, *54*, 370–378.
Fergason, R. L., P. R. Christensen, and H. H. Kieffer (2006), High-resolution thermal inertia derived from the Thermal Emission Imaging System (THEMIS): Thermal model and applications, *J. Geophys. Res.*, *111*, E12004, doi:10.1029/2006JE002735.
Garry, W. B., J. R. Zimbelman, and T. K. P. Gregg (2007), Morphology and emplacement of a long channeled lava flow near Ascraeus Mons Volcano, Mars, *J. Geophys. Res.*, *112*, E08007, doi:10.1029/2006JE002803.
Glaze, L. S., and S. M. Baloga (2006), Rheologic inferences from the levees of lava flows on Mars, *J. Geophys. Res.*, *111*, E09006, doi:10.1029/2005JE002585.
Glaze, L. S., S. W. Anderson, E. R. Stofan, S. Baloga, and S. E. Smrekar (2005), Statistical distribution of tumuli on pahoehoe flow surfaces: Analysis of examples in Hawaii and Iceland and potential applications to lava flows on Mars, *J. Geophys. Res.*, *110*, B08202, doi:10.1029/2004JB003564.
Greeley, R. (1973), Mariner 9 photographs of small volcanic structures on Mars, *Geology*, *1*, 175–180.
Greeley, R. (1977a), Volcanic morphology, in *Volcanism of the Eastern Snake River Plain, Idaho: A Comparative Planetary Geology Guidebook*, *NASA CR-154621*, edited by R. Greeley and J. S. King, pp. 5–22, NASA, Washington, D. C.
Greeley, R. (1977b), Basaltic "plains" volcanism, in *Volcanism of the Eastern Snake River Plain, Idaho: A Comparative Planetary Geology Guidebook*, *NASA CR-154621*, edited by R. Greeley and J. S. King, pp. 23–44, NASA, Washington, D. C.
Greeley, R. (1982), The Snake River Plain, Idaho: Representative of a new category of volcanism, *J. Geophys. Res.*, *87*(B4), 2705–2712.
Greeley, R. (1987), The role of lava tubes in Hawaiian volcanoes, in *Volcanism in Hawaii*, edited by R. W. Decker et al., *U.S. Geol. Surv. Prof. Pap.*, *1350*, 1589–1605.
Greeley, R., and P. D. Spudis (1981), Volcanism on Mars, *Rev. Geophys.*, *19*, 13–41.
Head, J. W., and D. R. Marchant (2003), Cold-based mountain glaciers on Mars: Western Arsia Mons, *Geology*, *31*(7), 641–644.
Head, J. W., W. B. Bryan, R. Greeley, J. E. Guest, P. H. Shultz, R. S. J. Sparks, G. P. L. Walker, J. L. Whitford-Stark, C. A. Wood, and M. H. Carr (1981), Distribution and morphology of basalt deposits on planets, in *Basaltic Volcanism on the Terrestrial Planets*, edited by W. M. Kaula et al., pp. 702–887, Pergamon, New York.
Head, J. W., L. Wilson, and K. L. Mitchell (2003), Generation of recent massive water floods at Cerberus Fossae, Mars by dike emplacement, cryospheric cracking, and confined aquifer groundwater release, *Geophys. Res. Lett.*, *30*(11), 1577, doi:10.1029/2003GL017135.
Heliker, C. C., M. T. Mangan, T. N. Mattox, J. P. Kauahikaua, and R. T. Helz (1998), The character of long-term eruptions: Inferences from episodes 50–53 of the Puu Oo-Kupaianaha eruption of Kilauea Volcano, *Bull. Volcanol.*, *59*, 381–393.
Hiesinger, H., J. W. Head III, G. Neukum, and the HRSC Co-Investigator Team (2005), Rheologic properties of late-stage lava flows on Ascraeus Mons: New evidence from HRSC, *Lunar Planet. Sci.* [CD-ROM], *XXXVI*, Abstract 1727.
Hiesinger, H., J. W. Head III, and G. Neukum (2007), Young lava flows on the eastern flank of Ascraeus Mons: Rheological properties derived from High Resolution Stereo Camera (HRSC) images and Mars Orbiter Laser Altimeter (MOLA) data, *J. Geophys. Res.*, *112*, E05011, doi:10.1029/2006JE002717.
Hodges, C. A., and H. J. Moore (1994), *Atlas of Volcanic Landforms on Mars*, *U.S. Geol. Surv. Prof. Pap.*, *1534*, 194 pp.
Holcomb, R. T. (1987), Eruptive history and long-term behavior of Kilauea Volcano, in *Volcanism in Hawaii*, edited by R. W. Decker et al., *U.S. Geol. Surv. Prof. Pap.*, *1350*, 261–350.
Hughes, S. S., S. E. H. Sakimoto, T. K. P. Gregg, and S. M. Brady (2005), Petrologic evidence for multiple, chemically evolved magma batches, and implications for plains volcanism on Earth and Mars, *Lunar Planet. Sci.* [CD-ROM], *XXXVI*, Abstract 2396.
Ivanov, M. A., and J. W. Head (2006), Alba Patera, Mars: Topography, structure, and evolution of a unique late Hesperian–early Amazonian shield volcano, *J. Geophys. Res.*, *111*, E09003, doi:10.1029/2005JE002469.
Kauahikaua, J., K. V. Cashman, T. N. Mattox, C. C. Heliker, K. A. Hon, M. T. Mangan, and C. R. Thornber (1998), Observations on basaltic lava streams in tubes from Kilauea volcano, Island of Hawaii, *J. Geophys. Res.*, *103*(B11), 27,303–27,323.
Kauahikaua, J., D. R. Sherrod, K. V. Cashman, C. Heliker, K. Hon, T. N. Mattox, and J. A. Johnson (2003), Hawaiian lava-flow dynamics during the Puu Oo-Kupaianaha eruption: A tale of two decades, in *The Puu Oo-Kupaianaha Eruption of Kilauea Volcano, Hawaii, the First 20 Years*, edited by C. Heliker et al., *U.S. Geol. Surv. Prof. Pap.*, *1676*, 63–87.
Keszthelyi, L. (1995), A preliminary thermal budget for lava tubes on the Earth and planets, *J. Geophys. Res.*, *100*(B10), 20,411–20,420.
Kreslavsky, M. A., and J. W. Head III (1999), Kilometer-scale slopes on Mars and their correlation with geologic units: Initial results from Mars Orbiter Laser Altimeter (MOLA) data, *J. Geophys. Res.*, *104*(E9), 21,911–21,924.
Kreslavsky, M. A., and J. W. Head III (2000), Kilometer-scale roughness of Mars: Results from MOLA data analysis, *J. Geophys. Res.*, *105*(E11), 26,695–26,711.
Leverington, D. W. (2004), Volcanic rilles, streamlined islands, and the origin of outflow channels on Mars, *J. Geophys. Res.*, *109*, E10011, doi:10.1029/2004JE002311.
Lockwood, J. P., and P. W. Lipman (1987), Holocene eruptive history of Mauna Loa Volcano, in *Volcanism in Hawaii*, edited by R. W. Decker et al., *U.S. Geol. Surv. Prof. Pap.*, *1350*, 509–536.
Longley, P. A., M. F. Goodchild, D. J. Maguire, and D. W. Rhind (2001), *Geographic Information Systems and Science*, 454 pp., John Wiley, New York.
Macdonald, G. A. (1956), Pahoehoe, aa, and block lava, *Am. J. Sci.*, *251*, 169–191.
Malin, M. C. (1980), Lengths of Hawaiian lava flows, *Geology*, *8*, 306–308.
Malin, M. C., and K. S. Edgett (2001), Mars Global Surveyor Mars Orbiter Camera: Interplanetary cruise through the primary mission, *J. Geophys. Res.*, *106*(E10), 23,429–23,570.
Malin, M. C., G. E. Danielson, A. P. Ingersoll, H. Masursky, J. Veverka, M. A. Ravine, and T. A. Soulanille (1992), The Mars Observer Camera, *J. Geophys. Res.*, *97*(E5), 7699–7718.
Masursky, H., et al. (1972), Mariner 9 television reconnaissance of Mars and its satellites: Preliminary results, *Science*, *175*, 294–305.

Masursky, H., A. L. Dial Jr., and M. H. Strobell (1978), Geologic map of the Phoenicis Lacus Quadrangle of Mars, scale 1:5,000,000, *U.S. Geol. Surv. Misc. Invest. Ser.*, *Map I-896 (MC-17)*.

McCauley, J. F., M. H. Carr, J. A. Cutts, W. K. Hartmann, H. Masursky, D. J. Milton, R. P. Sharp, and D. E. Wilhelms (1972), Preliminary Mariner report on the geology of Mars, *Icarus*, *17*, 289–327.

McEwen, A. S., et al. (2007), Mars Reconnaissance Orbiter's High Resolution Imaging Science Experiment (HiRISE), *J. Geophys. Res.*, *112*, E05S02, doi:10.1029/2005JE002605.

McGovern, P. J., and S. C. Solomon (1993), State of stress, faulting, and eruption characteristics of large volcanoes on Mars, *J. Geophys. Res.*, *98*(E12), 23,553–23,579.

Mège, D., and P. Masson (1996), A plume tectonics model for the Tharsis province, Mars, *Planet. Space Sci.*, *44*, 1499–1546.

Mellon, M. T., B. M. Jakosky, H. H. Kieffer, and P. R. Christensen (2000), High-resolution thermal inertia mapping from the Mars Global Surveyor Thermal Emission Spectrometer, *Icarus*, *148*, 437–455.

Moore, J. G., and R. K. Mark (1992), Morphology of the Island of Hawaii, *GSA Today*, *2*(11), 257–262.

Morgan, J. K., and P. J. McGovern (2005), Discrete element simulations of gravitational volcanic deformation: 1. Deformation structures and geometries, *J. Geophys. Res.*, *110*, B05402, doi:10.1029/2004JB003252.

Morris, E. C., and K. L. Tanaka (1994), Geologic maps of the Olympus Mons region of Mars, scale 1:2,000,000 and 1:1,000,000, *U.S. Geol. Surv. Misc. Invest. Ser.*, *Map I-2327*.

Mouginis-Mark, P. J. (1985), Volcano/ground ice interactions in Elysium Planitia, Mars, *Icarus*, *64*, 265–284.

Mouginis-Mark, P. J. (1990), Recent water release in the Tharsis region of Mars, *Icarus*, *84*, 362–373.

Mouginis-Mark, P. J. (2002), Prodigious ash deposits near the summit of Arsia Mons volcano, Mars, *Geophys. Res. Lett.*, *29*(16), 1768, doi:10.1029/2002GL015296.

Mouginis-Mark, P. J. (2003), New observations of the diversity of eruption styles along the SW rift zone of Arsia Mons, Mars, Abstract 3001 presented at Sixth International Conference on Mars, Lunar and Planet. Inst., Pasadena, Calif., 20–25 July.

Mouginis-Mark, P. J., and P. R. Christensen (2005), New observations of volcanic features on Mars from the THEMIS instrument, *J. Geophys. Res.*, *110*, E08007, doi:10.1029/2005JE002421.

Mouginis-Mark, P. J., L. Wilson, and M. T. Zuber (1992), The physical volcanology of Mars, in *Mars*, edited by H. H. Kieffer et al., pp. 424–452, Univ. of Ariz. Press, Tucson.

Neukum, G., and K. Hiller (1981), Martian ages, *J. Geophys. Res.*, *86*, 3097–3121.

Neukum, G., R. Jaumann, and the HRSC Co-Investigator and Experiment Team (2004a), HRSC: The High Resolution Stereo Camera of Mars Express, *Eur. Space Agency Spec. Publ.*, *ESA-SP 1240*, 17–36.

Neukum, G., et al. (2004b), Recent, episodic volcanic and glacial activity on Mars revealed by the High Resolution Stereo Camera, *Nature*, *432*, 971–979.

Nowicki, S. A., and P. R. Christensen (2007), Rock abundance on Mars from the Thermal Emission Spectrometer, *J. Geophys. Res.*, *112*, E05007, doi:10.1029/2006JE002798.

Parfitt, E. A., and J. W. Head (1993), Buffered and unbuffered dike emplacement on Earth and Venus: Implications for magma reservoir size, depth, and rate of magma replenishment, *Earth Moon Planets*, *61*, 249–281.

Parfitt, E. A., L. Wilson, and J. W. Head (1993), Basaltic magma reservoirs: Factors controlling their rupture characteristics and evolution, *J. Volcanol. Geotherm. Res.*, *55*, 1–14.

Peterson, D. W., R. T. Holcomb, R. I. Tilling, and R. L. Christiansen (1994), Development of lava tubes in the light of observations at Mauna Ulu, Kilauea Volcano, Hawaii, *Bull. Volcanol.*, *56*, 343–360.

Plescia, J. B. (2004), Morphometric properties of Martian volcanoes, *J. Geophys. Res.*, *109*, E03003, doi:10.1029/2002JE002031.

Plescia, J. B., and R. S. Saunders (1979), The chronology of the Martian volcanoes, in *Proceedings of the 10th Lunar and Planetary Science Conference*, pp. 2841–2859, Pergamon, New York.

Plescia, J. B., and R. S. Saunders (1982), Tectonic history of the Tharsis region, Mars, *J. Geophys. Res.*, *87*(B12), 9775–9791.

Pupysheva, N. V., A. T. Basilevsky, and B. A. Ivanov (2006), Lava tubes on the summit part of Olympus Mons volcano, Mars, and channel network at its south-east foot: Morphology, depths, widths, lengths, and coefficients of sinuosity, Abstract 71 presented at 44th Vernadsky-Brown Microsymposium on Comparative Planetology, Moscow, 9–11 Oct.

Rowland, S. K. (1996), Slopes, lava flow volumes, and vent distributions on Volcan Fernandina, Galapagos Islands, *J. Geophys. Res.*, *101*(B12), 27,657–27,672.

Rowland, S. K., and H. Garbeil (2000), Slopes of oceanic basalt volcanoes, in *Remote Sensing of Active Volcanism*, *Geophys. Monogr. Ser.*, vol. 116, edited by P. J. Mouginis-Mark et al., pp. 223–247, AGU, Washington, D. C.

Rowland, S. K., and G. P. L. Walker (1990), Pahoehoe and aa in Hawaii: Volumetric flow rate controls the lava structure, *Bull. Volcanol.*, *52*, 615–628.

Ruff, S. W., and P. R. Christensen (2002), Bright and dark regions on Mars: Particle size and mineralogical characteristics based on Thermal Emission Spectrometer data, *J. Geophys. Res.*, *107*(E12), 5127, doi:10.1029/2001JE001580.

Sakimoto, S. E. H., and M. T. Zuber (1998), Flow and convection cooling in lava tubes, *J. Geophys. Res.*, *103*(B11), 27,465–27,487.

Sakimoto, S. E. H., J. Crisp, and S. M. Baloga (1997), Eruption constraints on tube-fed planetary lava flows, *J. Geophys. Res.*, *102*(E3), 6597–6614.

Sakimoto, S. E. H., T. K. P. Gregg, S. S. Hughes, and J. Chadwick (2003), Martian plains volcanism in Syria Planum and Tempe Mareotis as analogs to the Eastern Snake River Plains, Idaho: Similarities and possible petrologic contributions to topography, *Lunar Planet. Sci.* [CD-ROM], *XXXIV*, Abstract 1740.

Schneeberger, D. M., and D. C. Pieri (1991), Geomorphology and stratigraphy of Alba Patera, Mars, *J. Geophys. Res.*, *96*, 1907–1930.

Schupack, B. B., and S. E. H. Sakimoto (2006), Eruption styles of small Martian shield volcanoes and indications of post flow tectonic deformation on Syria Planum, from MOLA, TES, and THEMIS data, *Lunar Planet. Sci.* [CD-ROM], *XXXVII*, Abstract 1157.

Scott, D. H., and M. H. Carr (1978), Geologic map of Mars, scale 1:25,000,000, *U.S. Geol. Surv. Misc. Invest. Ser.*, *Map I-1083*.

Scott, D. H., and K. L. Tanaka (1981a), Map showing lava flows in the northeast part of the Phoenicis Lacus Quadrangle of Mars, scale 1:2,000,000, *U.S. Geol. Surv. Misc. Invest. Ser.*, *Map I-1277 (MC-17 NE)*.

Scott, D. H., and K. L. Tanaka (1981b), Map showing lava flows in the southeast part of the Amazonis Quadrangle of Mars, scale 1:2,000,000, *U.S. Geol. Surv. Misc. Invest. Ser.*, *Map I-1280 (MC-8 SE)*.

Scott, D. H., and K. L. Tanaka (1986), Geologic map of the western equatorial region of Mars, scale 1:15,000,000, *U.S. Geol. Surv. Misc. Invest. Ser.*, *Map I-1802-A*.

Scott, D. H., and J. R. Zimbelman (1995), Geologic map of Arsia Mons, Mars, scale 1:1,000,000, *U.S. Geol. Surv. Misc. Invest. Ser.*, *Map I-2480*.

Scott, D. H., G. G. Schaber, and K. L. Tanaka (1981a), Map showing lava flows in the southeast part of the Tharsis Quadrangle of Mars, scale 1:2,000,000, *U.S. Geol. Surv. Misc. Invest. Ser.*, *Map I-1269 (MC-9 SE)*.

Scott, D. H., G. G. Schaber, K. C. Horstman, A. L. Dial Jr., and K. L. Tanaka (1981b), Map showing lava flows in the northwest part of the Phoenicis Lacus Quadrangle of Mars, scale 1:2,000,000, *U.S. Geol. Surv. Misc. Invest. Ser.*, *Map I-1272 (MC-17 NW)*.

Scott, D. H., G. G. Schaber, K. C. Horstman, A. L. Dial Jr., and K. L. Tanaka (1981c), Map showing lava flows in the southwest part of the Tharsis Quadrangle of Mars, scale 1:2,000,000, *U.S. Geol. Surv. Misc. Invest. Ser.*, *Map I-1268 (MC-9 SW)*.

Scott, D. H., J. M. Dohm, and J. R. Zimbelman (1998), Geologic map of Pavonis Mons Volcano, Mars, scale 1:1,000,000, *U.S. Geol. Surv. Misc. Invest. Ser.*, *Map I-2561*.

Scott, E. D., and L. Wilson (1998), Evidence for fluvial features produced by sill emplacement on the upper flanks of Ascraeus Mons Volcano, Mars, *Lunar Planet. Sci.*, *XXVIV*, Abstract 1355.

Scott, E. D., and L. Wilson (1999), Evidence for a sill emplacement on the upper flanks of the Ascraeus Mons shield volcano, Mars, *J. Geophys. Res.*, *104*(E11), 27,079–27,089.

Shean, D. E., J. W. Head III, J. L. Fastook, and D. R. Marchant (2007), Recent glaciation at high elevations on Arsia Mons, Mars: Implications for the formation and evolution of large tropical mountain glaciers, *J. Geophys. Res.*, *112*, E03004, doi:10.1029/2006JE002761.

Smith, D., G. Neumann, R. E. Arvidson, E. A. Guinness, and S. Slavney (2003), Mars Global Surveyor Laser Altimeter Mission Experiment Gridded Data Record, *MGS-M-MOLA-5-MEGDR-L3-V1.0*, NASA Planet. Data Syst., Washington, D. C.

Smith, D. E., et al. (1999), The global topography of Mars and implications for surface evolution, *Science*, *284*, 1495–1503.

Smith, D. E., et al. (2001), Mars Orbiter Laser Altimeter: Experiment summary after the first year of global mapping of Mars, *J. Geophys. Res.*, *106*(E10), 23,689–23,722.

Swanson, D. A. (1973), Pahoehoe flows from the 1969–1971 Mauna Ulu eruption, Kilauea Volcano, Hawaii, *Geol. Soc. Am. Bull.*, *84*, 615–626.

Tanaka, K. L., M. P. Golombek, and W. B. Banerdt (1991), Reconciliation of stress and structural histories of the Tharsis region of Mars, *J. Geophys. Res.*, *96*(E1), 15,617–15,633.

Thomas, P. J., S. W. Squyres, and M. H. Carr (1990), Flank tectonics of Martian volcanoes, *J. Geophys. Res.*, *95*, 14,345–14,355.

Walker, G. P. L. (1999), Volcanic rift zones and their intrusion swarms, *J. Volcanol. Geotherm. Res.*, *94*, 21–34.

Wentworth, C. K., and G. A. Macdonald (1953), Structures and forms of basaltic rocks in Hawaii, *U.S. Geol. Surv. Bull.*, *994*, 1–90.

Werner, S. (2005), Major aspects of the chronostratigraphy and geologic evolutionary history of Mars, Ph.D. dissertation, Free Univ., Berlin. (Available at http://www.diss.fu-berlin.de/2006/33/index.html)

Whitford-Stark, J. L. (1982), Factors influencing the morphology of volcanic landforms: An Earth-Moon comparison, *Earth Sci. Rev.*, *18*, 109–168.

Williams, D. A., R. Greeley, E. Hauber, K. Gwinner, and G. Neukum (2005), Erosion by flowing Martian lava: New insights for Hecates Tholus from Mars Express and MER data, *J. Geophys. Res.*, *110*, E05006, doi:10.1029/2004JE002377.

Wilson, L., and J. W. Head III (2002), Tharsis-radial graben systems as the surface manifestation of plume-related dike intrusion complexes: Models and implications, *J. Geophys. Res.*, *107*(E8), 5057, doi:10.1029/2001JE001593.

Wilson, L., and P. J. Mouginis-Mark (1984), Martian sinuous rilles (abstract), *Lunar Planet. Sci.*, *XV*, 926–927.

Wilson, L., and P. J. Mouginis-Mark (2001), Estimation of volcanic eruptions conditions for a large flank event on Elysium Mons, Mars, *J. Geophys. Res.*, *106*(E9), 20,621–20,628.

Wilson, L., E. D. Scott, and J. W. Head (2001), Evidence for episodicity in the magma supply to the large Tharsis volcanoes, *J. Geophys. Res.*, *106*(E1), 1423–1433.

Wolfe, E. W., W. S. Wise, and G. B. Dalrymple (1997), The geology and petrology of Mauna Kea Volcano, Hawaii–A study of postshield volcanism, *U.S. Geol. Surv. Prof. Pap.*, *1557*, 129 pp.

Zimbelman, J. R. (1985), Estimates of rheologic properties for flows on the Martian volcano Ascraeus Mons, *Proc. Lunar Planet. Sci. Conf. 16th*, part 1, *J. Geophys. Res.*, *90*, suppl., D157–D162.

Zimbelman, J. R. (1998), Emplacement of long lava flows on planetary surfaces, *J. Geophys. Res.*, *103*(B11), 27,503–27,516.

J. E. Bleacher, Planetary and Geodynamics Laboratory, NASA Goddard Space Flight Center, Code 698, Building 33, Room G310, Greenbelt, MD 20771, USA. (jake@puuoo.gsfc.nasa.gov)

S. R. Cave, R. Greeley, and D. A. Williams, School of Earth and Space Exploration, Arizona State University, Tempe, AZ 85287, USA.

G. Neukum, Institute of Geological Sciences, Freie Universitaet, Malteserstrasse 74-100, D-12249 Berlin, Germany.